This article was downloaded by:
On: *25 January 2011*
Access details: *Access Details: Free Access*
Publisher *Taylor & Francis*
Informa Ltd Registered in England and Wales Registered Number: 1072954 Registered office: Mortimer House, 37-41 Mortimer Street, London W1T 3JH, UK

Separation Science and Technology
Publication details, including instructions for authors and subscription information:
http://www.informaworld.com/smpp/title~content=t713708471

Role of Foulant-Membrane Interactions in Organic Fouling of RO Membranes with Respect to Membrane Properties

Juhee Yang[a]; Sangyoup Lee[a]; Youngbeom Yu[a]; Jihun Kuk[a]; Seungkwan Hong[a]; Seungyoon Lee[b]; Kyungsok Min[c]
[a] Department of Civil, Environmental & Architectural Engineering, Korea University, Seoul, Korea [b] K-water Research Institute (KRI), Korea Water Resources Corporation, Daejon, Korea [c] Department of Environmental Engineering, Kyungpook National University, Daegu, Korea

Online publication date: 23 April 2010

To cite this Article Yang, Juhee , Lee, Sangyoup , Yu, Youngbeom , Kuk, Jihun , Hong, Seungkwan , Lee, Seungyoon and Min, Kyungsok(2010) 'Role of Foulant-Membrane Interactions in Organic Fouling of RO Membranes with Respect to Membrane Properties', Separation Science and Technology, 45: 7, 948 — 955
To link to this Article: DOI: 10.1080/01496391003659911
URL: http://dx.doi.org/10.1080/01496391003659911

PLEASE SCROLL DOWN FOR ARTICLE

Full terms and conditions of use: http://www.informaworld.com/terms-and-conditions-of-access.pdf

This article may be used for research, teaching and private study purposes. Any substantial or systematic reproduction, re-distribution, re-selling, loan or sub-licensing, systematic supply or distribution in any form to anyone is expressly forbidden.

The publisher does not give any warranty express or implied or make any representation that the contents will be complete or accurate or up to date. The accuracy of any instructions, formulae and drug doses should be independently verified with primary sources. The publisher shall not be liable for any loss, actions, claims, proceedings, demand or costs or damages whatsoever or howsoever caused arising directly or indirectly in connection with or arising out of the use of this material.

Separation Science and Technology, 45: 948–955, 2010
Copyright © Taylor & Francis Group, LLC
ISSN: 0149-6395 print/1520-5754 online
DOI: 10.1080/01496391003659911

Taylor & Francis
Taylor & Francis Group

Role of Foulant-Membrane Interactions in Organic Fouling of RO Membranes with Respect to Membrane Properties

Juhee Yang,[1] Sangyoup Lee,[1] Youngbeom Yu,[1] Jihun Kuk,[1] Seungkwan Hong,[1] Seungyoon Lee,[2] and Kyungsok Min[3]

[1]*Department of Civil, Environmental & Architectural Engineering, Korea University, Seoul, Korea*
[2]*K-water Research Institute (KRI), Korea Water Resources Corporation, Daejon, Korea*
[3]*Department of Environmental Engineering, Kyungpook National University, Daegu, Korea*

Initial fouling behavior due to membrane-foulant interactions was investigated by atomic force microscopy for various reverse osmosis membranes with different surface properties. Carboxylate modified latex and unmodified latex particles were used as surrogates of organic foulants. The results showed that the membrane-foulant adhesion forces were mainly governed by membrane surface properties such as hydrophobicity and surface charge. Stronger adhesion forces were determined for the membranes with more hydrophobic and less surface charge. Fouling experiments were further carried out to correlate the adhesion force data to actual flux-decline curves. A remarkable correlation was obtained where the membranes with stronger adhesion force more suffered from flux decline.

Keywords adhesion force; Atomic Force Microscopy; membrane surface property; organic fouling; RO membrane

Downloaded At: 08:48 25 January 2011

INTRODUCTION

Reverse Osmosis (RO) membrane filtration has been taken as the most promising technology in the water treatment system and has developed significantly over the past few decades. A great number of filtration systems were applied to special (i.e., seawater desalination and wastewater reuse) and even general water treatment fields since the world suffered from water scarcity. Although the membrane filtration systems have been expected as the most feasible alternative for water treatment, several problems have remained for the efficient operation of membrane filtration. The major challenge of the membrane system is the membrane fouling caused by various foulants such as particle, organic, bio, and scaling. According to earlier studies, there are several factors affecting membrane fouling such as the membrane surface characteristics, the solution chemistry of feed water, and the foulant properties (1). Among these factors, the solution chemistry and the foulant properties are non-selective factors while the membrane surface characteristics are the selective factors. The filtration efficiency differs according to the membrane surface characteristics since most organic foulants are negatively charged and, thus the electrostatic repulsion between evenly charged foulants and membrane surface determines the extent of membrane fouling.

According to the previous studies (2–4), pore blocking does not play an important role in RO membrane fouling since RO membranes are most considered to be nonporous and, thus, foulant adhesion on the membrane surface mainly controls membrane fouling. Therefore, depending on the adhesion force between the membrane surface and foulants, the initial fouling rate can be determined. It means that the quantification of intermolecular interactions between foulants and membrane would be a promising tool to elucidate the intermolecular interaction, thus providing proper options for efficient fouling control (5,6). This adhesion force is greatly affected by the characteristics of the functional groups of the membrane surface and foulants. The membrane fouling can be divided into two steps. The first step is the foulant adsorption on the clean membrane surface, which is defined as "membrane-foulant interaction" (i.e., initial rapid fouling). The fouling rate of the first step is decisive in overall efficiency. The next step is the foulants' accumulation on the fouled membrane surface, which is defined as "foulant–foulant interaction," and this step holds the greater part of the fouling mechanism (i.e., long-term gradual fouling). Between two steps of membrane fouling, "membrane-foulant interaction" is mainly affected by the membrane surface property and usually determines the initial fouling rate, while the "foulant–foulant interaction" is not clearly distinguishable with respect to the membrane surface property as the clean membrane surface has already been covered by lots of foulants due to the initial membrane-foulant interaction.

Received 1 November 2009; accepted 1 December 2009.
Address correspondence to Seungkwan Hong, Department of Civil, Environmental & Architectural Engineering, Korea University, 1, 5-ka, Anam-Dong, Sungbuk-Gu, Seoul 136-713, Korea. Tel.: +82-2-3290-3322. E-mail: skhong21@korea.ac.kr

Downloaded At: 08:48 25 January 2011

Atomic Force Microscopy (AFM) was initially developed as an imaging tool with atomic-level resolution. AFM also allows to directly quantity the surface forces as well as the molecular forces. Most previous researchers measured only the interaction force between the silicon tip and the surface with different materials. However, recently, not only the spherical particle but also the nano to micro-scale microorganism attachment to the cantilever tip becomes possible. Therefore, we focused on the interaction force between the particle (i.e., foulant probe) and the membrane surface with different surface properties under the fixed solution chemistries. Systematic and rigorous characterizations of RO membranes provided useful insight into the better understanding of fouling phenomena, leading to an efficient control of membrane fouling.

In this study, the most widely used commercial RO membranes were characterized under fixed solution chemistries (i.e., pH 5.5, Temp. 25°C, and TDS 10 mg/L). Both the chemical and the physical properties of the membrane surface were investigated. The chemical properties including surface charge and hydrophobicity were determined by using zeta potential and contact angle measurement, respectively. The physical property including surface roughness was analyzed by using AFM in conjunction with an image analysis system (7). Later, the interaction force between the foulant probes (i.e., carboxylic modified latex (CML) particles and unmodified latex particles) and commercial RO membrane surface with different properties were measured. Lastly, the flux tests were performed with varying the concentration of organic foulants (i.e., alginate; $2-500$ mg/L). The operation time was adjusted to 70 hours (low concentration of organic) and 300 minutes (high concentration of organic) applying the same solution chemistries for force measurement. The main purpose of this study is to see whether the membrane surface properties have a correlation with the interaction force and to elucidate the relationship between the foulant-membrane adhesions and the actual flux decline rate. The results obtained in this study are expected to provide useful guidelines for selecting suitable membrane to real RO applications.

MATERIALS AND METHODS

RO Membranes

Three commercial RO membranes were used in this study. The RO membranes were Toray TM-820 (Chiba, Japan), Hydranautics SWC-5 (Oceanside, CA), and Dow-Filmtec SW-30HR (Minneapolis, MA). All membranes were composed of polyamide thin film with an average salt rejection over 99.5%. All membranes were stored in deionized (DI) water at 4°C and the water was replaced regularly prior to the experiments. The membranes were first characterized under the conventional conditions (i.e., pH 5.5, Temp. 25°C, TDS 10 mg/L) for chemical and physical properties such as surface roughness, zeta potential, and contact angle. The results are summarized in Table 1, where the surface characteristics of each membrane are quite different. It is also shown in Fig. 1 that the morphological surface image of each membrane varies substantially.

Solution Chemistry

The characterization of the membrane surface including AFM, zeta potential, and contact angle measurement was performed in the test solution (i.e., pH 5.5, Temp. 25°C, TDS 10 mg/L). The test solution pH was adjusted to 5.5 using 0.1 M of NaOH or HCl stock solutions and the TDS value of 10 mg/L was employed where NaCl was used for TDS adjustment.

Membrane Surface Characterization

Surface Roughness

The membrane surface was scanned by AFM imaging analysis (PUCOStation AFM, Surface Imaging Systems, Herzogenrath, Germany). Liquid phase AFM imaging was performed in contact mode with SiN probes whose backside has 30 nm thick aluminium reflex coating for better resolution and stability in liquid phase application (APPNANO, Applied Nano Structures, Inc., Santa Clara, CA). The probes have a spring constant of 0.1 N/m (±0.08 N/m), resonance frequency of 28 kHz (±10 kHz), tip radius of $5\sim6$ nm, tip height of 14 μm (±2 μm), and a cantilever length of 225 μm (±10 μm). The membrane was immersed in a petri dish containing test solution for

TABLE 1
Surface characteristics of the membranes investigated under ambient conditions[a]

Membrane	RMS roughness (nm)	Surface charge[b] (mV)	Contact angle (°)
TM-820	53.57	−13.98	72.20
SWC-5	127.23	−18.04	72.30
SW-30HR	87.65	−24.01	24.90

[a]Test solution conditions: pH = 5.5, Temperature = 25°C, and TDS = 10 mg/L NaCl.
[b]Zeta potential was determined at a background electrolyte concentration of 10 mM KCl.

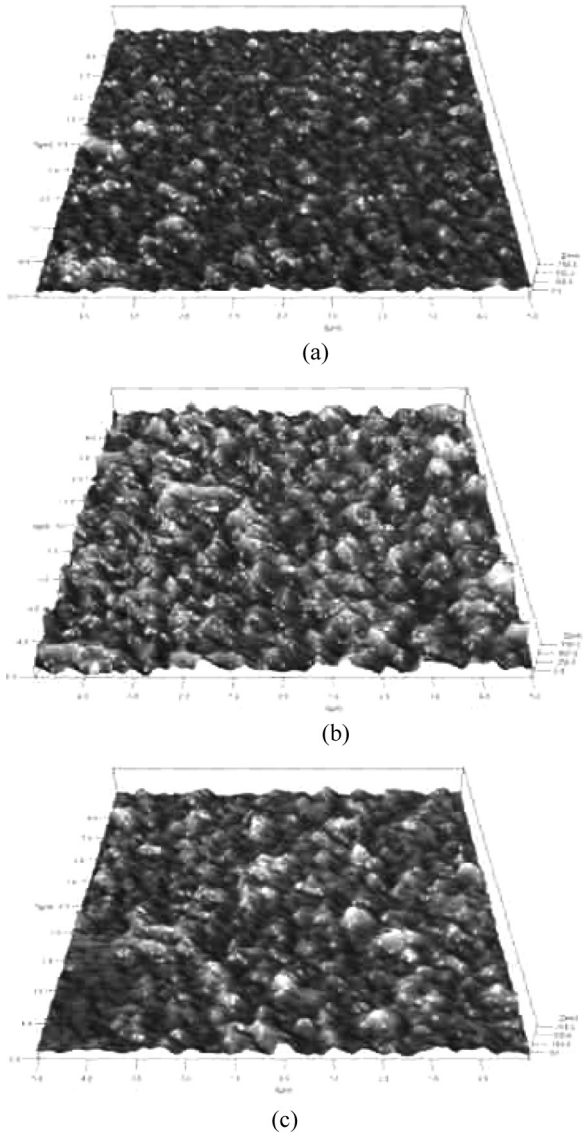

FIG. 1. AFM images of (a) TM-820, (b) SWC-5, and (c) SWC-5. Measurement was performed in liquid phase at pH 7.0, TDS 10 mg/L, and temperature was 25°C.

10 minutes to make a stable condition. Surface scanning was then initiated by approaching the cantilever to the membrane surface.

All membranes were scanned several times with randomly varying a scan position. The roughness value was quantified by the root mean square (RMS) roughness, which is the RMS deviation of the peaks and valleys from the mean plane. The loading force ranged from 4.0 to 6.0 N/m with a scan speed of 0.7 line/sec and a scan area of $10 \times 10\,\mu m$. The scanned images were analyzed using SPIP software (Surface Imaging Systems, Herzogenrath, Germany). Each image was flattened by a baseline prior to roughness analysis.

Contact Angle

The goniometer (DM 500, Kyowa interface Science, Japan) with the droplet method was used for the measurement of the contact angle. Equilibrium contact angle was the average of the left and right contact angles (8). Ten measurements for each membrane were carried out with the same test solution. The reported values are the average of ten equilibrium contact angles.

Zeta Potential

The membrane zeta potential was determined by a streaming current electrokinetic analyzer (SurPass, Anton Paar GmbH, Graz, Austria) following the procedure described by Luxbacher (9). The zeta potential value was calculated by the Fairbrother and Mastin substitution. For the surface zeta potential analysis, 0.01 M KCl was used as a background electrolyte solution and the solution pH was varied from 2 to 10. The operating pressure ranged from 0 to 500 milibar (mbar) and the temperature was about 25°C.

Interaction Force Measurement

Model Foulant

Carboxylic functional groups are the predominant functional groups of organic matters. A CML particle (Interfacial Dynamics Corp., Portland, OR) was used as a surrogate for organic matter. A polystyrene latex particle (Duke Scientific Corp., Palo Alto, CA) was also used in making colloidal probes for the comparative study. Both CML and unmodified latex particles showed a nominal diameter of 4 μm (±0.033 μm). The former particle is hydrophilic, exhibits a negative charge, and has a porous surface. The latter particle is hydrophobic, exhibits a neutral charge, and has a glabrous surface. Visible differences in particle surface are shown in Figs. 2(a) and 2(c).

Colloidal Probes

Colloidal probes were made by attaching a spherical latex particle or CML particle with Scotch-Weld epoxy adhesive (3 M Industrial Adhesive and Tapes, St, Paul, MN) to AFM tip-less cantilever. Force measurement was performed in contact mode with SiN probes whose backside has an Au reflex coating for better resolution and stability in liquid phase application (APPNANO, Applied Nano Structures, Inc., Santa Clara, CA). The probes have a spring constant of 0.1 N/m (±0.08 N/m), resonance frequency of 28 kHz (±10 kHz), and cantilever length of 225 μm (±10 μm). The attachment procedure following the procedures described by Li and Elimelech was carried out on the micromanipulator and real time monitored through an extra powerful microscope. The spherical latex particle and CML particle were dropped on a cleaved mica surface and dried in a desiccator. Using the micromanipulator, a small dose glue spread on

Downloaded At: 08:48 25 January 2011

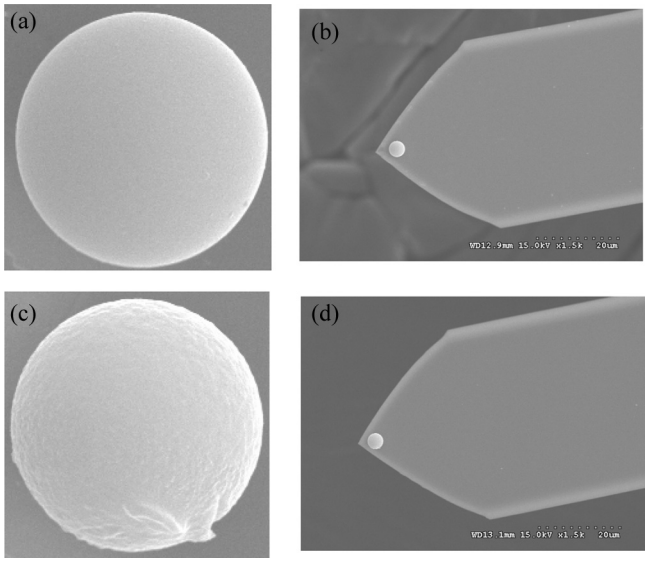

FIG. 2. SEM images of (a) surface of latex particle, (b) glued latex particle on the SiN tip, (c) surface of CML particle, and (d) glued CML particle on the SiN tip (both particles have 4 μm diameter).

Downloaded At: 08:48 25 January 2011

the mica surface covers the end of the tip-less cantilever and, then picks up a single sphere. After attaching the particle, the colloidal probe cured under UV light for 30 minutes. The completed colloidal probes with CML and latex particles are displayed in Figs. 2(b) and 2(d).

Force Measurement

The AFM allows the measurement of the force between the colloid probe and a membrane surface as a function of the displacement of the sample, where the sample displacement is varied using a piezoelectric crystal. A laser beam reflected from the back of the cantilever detects small changes in the deflection of the cantilever. The spring constant of the cantilever is necessary to convert the deflection to a force and to define the zero of force. Force measurement was randomly performed at five different locations on a $10\,\mu m \times 10\,\mu m$ area. The force measurements were conducted at minimum five different locations on the membrane, and 10 force measurements were taken at each location. To study the adhesion force due to the membrane–foulant interaction, only the retracting force curves were processed and converted to obtain the force versus surface-to-surface separation curves. The adhesion forces presented in this paper were the averages of all the adhesion forces determined at different locations. The force curves presented here were the representative force curves determined by averaging each force curve obtained at different locations.

Bench Scale Flux Test

The laboratory-scale cross flow RO membrane test unit was used in fouling experiments. Feed water solution chemistry was the same as that employed during AFM force measurements (i.e., pH 6.7, Temp 23°C, and TDS 10 mM). Commercial alginate (alginic acid sodium salt from brown algae, Sigma-Aldrich) was used as a model organic foulant, and two different foulant concentrations of 2 mg/L and 500 mg/L were tested. Operating time was differently applied according to the concentration of the foulant. Filtration time for the low and high foulant concentrations was 70 hours and 300 minutes, respectively, where a relatively short filtration time for the high foulant concentration was enough for full coverage of membrane surface by the foulants. Other experimental conditions were kept constant for all fouling runs (i.e., initial flux $= 12.75\,\mu m/s$, ?P $= 15 \sim 20$ bar, and temp. $= 20°C$).

RESULTS AND DISCUSSION

AFM Force Measurements Using Colloidal Probes

Latex and CML particle were utilized as colloidal probes for measuring the interaction force. The latex particles which represented a neutral charge were compared to the CML particle as a controlled group. The CML particle contains a highly negative charged layer of carboxylate functional groups, thereby serving as a surrogate for carboxylate rich foulants, such as humic acid and alginate. The adhesion forces between the foulant and the clean membrane surface determine the initial fouling rate since the membrane surface is clean during the initial stage of fouling. The adhesion forces between the foulant and the membrane are measured over a wide range of membrane surface to prevent substantial deviation of the interaction force due to the rough surface of the membrane. This indicates that the membrane surface morphology could greatly influence the foulant-membrane interactions (10). The deflection-distance curves shown in Fig. 3 were obtained during the retraction of the foulant probe from the membrane surface and, thus, the measure of the intermolecular adhesion forces (5,11,12). By measuring the interaction force at different locations of the membrane surface, the average adhesion force can be determined. In this study, the average adhesion force for different RO membranes were compared with respect to membrane surface characteristics including the surface charge, hydrophobicity, and roughness. Consequently, the influence of the membrane surface characteristics on foulant-membrane interaction (i.e., initial fouling tendency) was delineated.

Interaction Between Unmodified Latex Particle and Membranes

The results from the interaction force measurement for the latex probe are shown in Fig. 4. This graph is converted from deflection to force depending on the cantilever spring constant. As shown in Fig. 4, the SWC-5 membrane exhibits the strongest interaction force followed by the

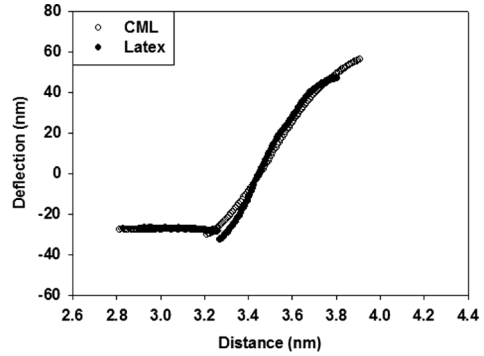

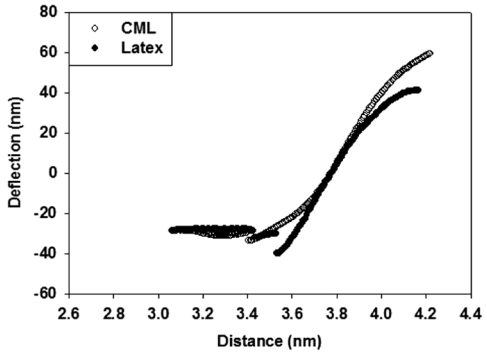

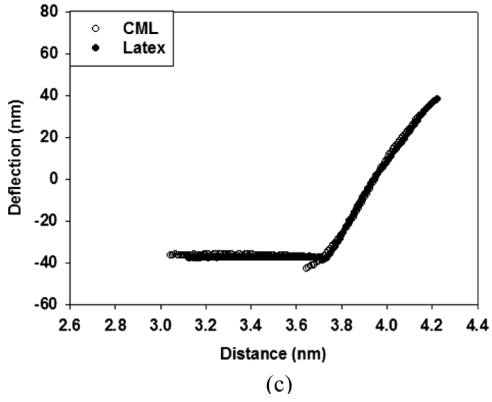

FIG. 3. Deflection versus distance curves obtained from force measurements: (a) TM-820, (b) SWC-5, and (c) SW-30HR (the only retracting curves are represented).

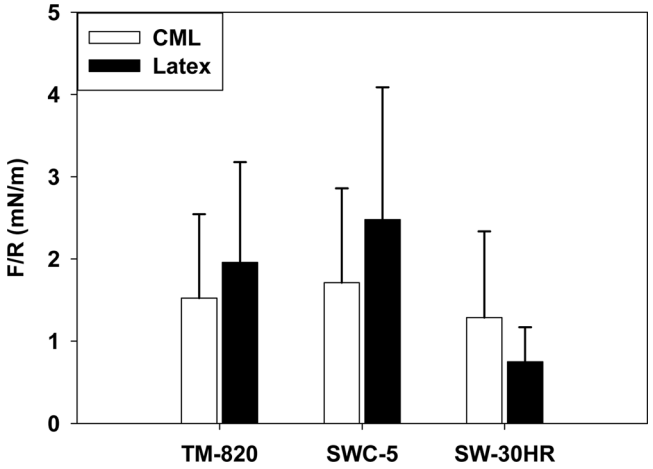

FIG. 4. Adhesion forces determined by the unmodified latex and CML particle probes for three RO membranes (pH 6.7, TDS 10 mM, and Temp 23°C).

TM-820 and SW-30HR. The SW-30HR membrane shows the relatively weak interaction force. Latex particles possess the almost neutral charge at DI water pH where the membrane surface mostly exhibits negative surface charge. One of the membranes, SW-30HR, is the most negatively charged which induces more electro-double layer repulsion against the foulant probes. In addition to the surface charge effect, the hydrophobicity is also an affecting factor to the adhesion force. The hydrophobic surface of the latex particle shows the stronger adhesion force on the hydrophobic surface than the hydrophilic surface. When the foulant and membrane surface have the same hydrophobicity, both surfaces are prone to cling to each other. As the results show, the latex particle has the weakest adhesion force in the SW-30HR. The effect of roughness is not clearly interpreted since the membrane surface heterogeneity is not uniform and randomly selected measuring points could be the prominence or depression. A successive detaching step in the force value is observed in Fig. 3(b). Some previous studies also found a similar detaching step; however, the succession step is not shown in all cases. It can be interpreted in terms of polymer chains and bond rupture or fracture mechanisms in bulk or at interfaces. As our result, the SWC-5 membrane has not only the highest roughness but also the most heterogeneity through the determining method of surface heterogeneity studied in previous research (7). Because the SWC-5 membrane owns the bunch of protrusions rather than others, it is supposed that the compensated particle bump into the surface. Through the difference of adhesion force according to the surface roughness and heterogeneity, we could determine that the membrane heterogeneity is influential property as well as the surface charge and hydrophobicity.

Interaction Between CML Particle and Membranes

The force measurements were conducted at pH 6.7 and TDS 10 mM solution, where the interaction forces between the CML particle and the clean membrane surface were measured. The CML particle can simulate the real organic fouling mechanism in the membrane system since the CML particle is coated with carboxylic groups and, then this particle has the hydrophilic property and negatively charged. As shown in Fig. 4, the entire force by the CML particle is less strong than by latex particle due to the electro double layer repulsion between the charged CML particle and membrane surface. However, SW-30HR has a stronger

Downloaded At: 08:48 25 January 2011

interaction force by the CML particle than by the latex particle. As interpreted in part by the interaction force of the latex particle, the hydrophilic CML particle has a stronger adhesion force with SW-30HR which has also the hydrophilic surface. It is very clearly divided into the reverse trend according to the hydrophobicity. For the interaction force with the CML probe, SWC-5 exhibits the strongest force followed by TM-820 and SW-30HR, which is closely related to the membrane surface charge. SWC-5 exhibits a less negative charge as −13.98 mV and the surface charge of SW-30HR is −24.01 mV. The more negatively charged surface showed the more powerful electro double layer repulsion. Therefore, the weakest adhesion appeared in case of the highly negative charged membrane such as SWC-5. By using the interaction force measurement, we can predict which membrane is more susceptible to fouling. Therefore, the interaction force regarding to the membrane surface properties can be a worthy indicator of membrane fouling propensity during cross-flow filtration (12). A relevancy between the membrane surface properties and interaction force will be explained in the next section.

Determination of Initial Flux-Decline Rate

As previously stated, the interaction force can be used as a fouling indicator. A bench-scale flux test was performed to verify a prediction through the interaction force. To apply the similar condition with adhesion force, aliginic acid was used as an organic surrogate. Water system generally contains about 2 mg/L concentration of organic compounds so the bench-scale flux test was performed with alginic acid 2 mg/L during 70 hours to check up the total flux decline. The fouling phenomenon is divided into two steps (i.e., initial rapid fouling and later long-term fouling) which have different mechanisms. The former is caused by membrane–foulant interaction and the latter by foulant–foulant interaction. It is supposed that the interaction force between the clean membrane surface and the foulant plays a significant role in the fouling mechanism, so, finding the initial flux decline is quite important in the determination of total fouling. As shown in the Fig. 5(a), all of the membranes have similar decrease in the flux through the total operation time. Through this flux test, (i.e., alginic acid 2 mg/L) the clear flux decline trend could not be distinguished, so an extremely high concentration of organic was applied in the flux test. The concentration alginic acid in feed water was changed to 500 mg/L to find out the dramatic initial flux decline. Flux decline is accelerated when the concentration of foulant is high and the initial flux decline happens due to the membrane-foulant adhesion. When the flux declines about 15 ~ 20% of initial flux, the chemical cleaning is performed in the real RO plant and, thus, the foulant–foulant interaction is not quite considerable in the real system. As a result, we focus on the membrane-fouling (i.e., initial fouling step) interaction.

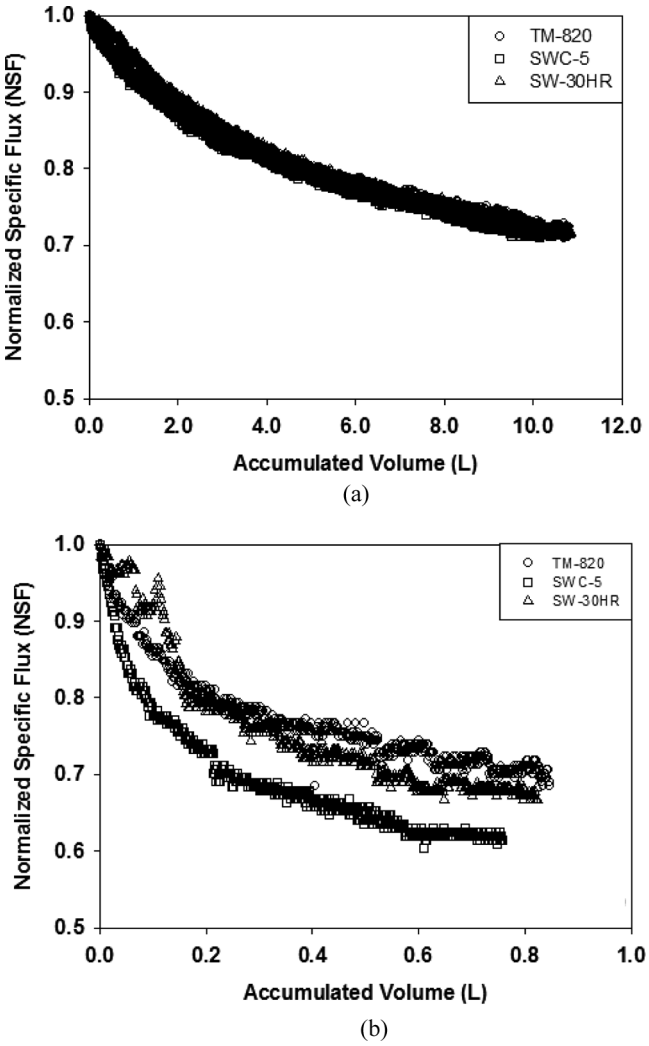

FIG. 5. Total flux data represented as normalized specific flux versus accumulation permeate volume. Feed water alginic acid concentration is (a) 2 mg/L and (b) 500 mg/L.

Initial fouling behaviors could be different with respect to membrane surface properties since the surface properties play an important role in the membrane-foulant interaction. As shown in Fig. 5(b), SWC-5 has the lowest flux at the end of the fouling run, and the following order is SW-30HR, and TM-820. The initial flux-decline trend (i.e., foulant-membrane interaction), however, has a different order like SWC-5, TM-820, and SW-30HR. This will be discussed in a subsequent sub-section along with the correlation results between the flux-decline rate and the adhesion force.

Relating Adhesion Force to Initial Flux-Decline Rate

The only measured interaction force by CML particle can be compared with the bench-scale flux test in Fig. 6. When the particle has the negative charge on the surface, the interaction force value has the same trend with the

Downloaded At: 08:48 25 January 2011

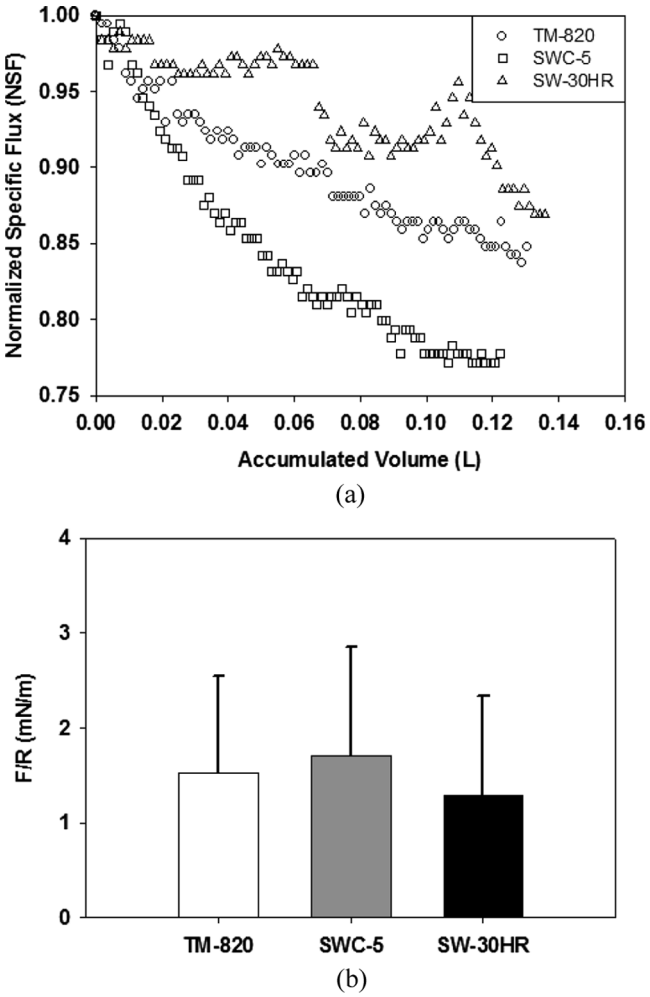

FIG. 6. Comparison of initial flux and interaction force: (a) initial fouling step (i.e., membrane-foulant interaction) by high concentration of alginic acid and (b) interaction force by CML particle.

charge of the membrane surface than the hydrophobicity order of SWC-5, TM-820, and SW-30HR. It has been considered that the initial fouling trend can be predicted through the interaction force between the clean membrane surface and foulant. Values of the interaction force contribute to interference between the clean membrane surface and the foulant while the fouling mechanism includes two steps such as the membrane-foulant interaction and the foulant–foulant interaction. Since the membrane chemical cleaning is performed when the flux dropped about 15% to 20% of the initial flux, the membrane-foulant interaction is a key mechanism in determining the initial flux decline rate. Therefore, the trend of total flux decline does not exactly match with the interaction force tendency since not only membrane-foulant interaction but also foulant–foulant interaction affect membrane fouling through the entire flux test. However, the initial fouling step exactly corresponds to the adhesion force value by AFM since both the adhesion force and the membrane-foulant interaction could be interpreted as the same mechanism.

CONCLUSION

Measurements of interaction force between the membrane surface and foulant were conducted to elucidate the relation between the flux decline rate and the interaction force for an efficient operating of the RO membrane system. There are several factors which determine the membrane system efficiency, for example membrane surface properties, solution chemistry, and foulant properties. Among those factors, only the membrane surface properties are selective factors since the feed water qualities can be changed according to the seasons or circumstance.

In our study, latex particle neutral surface charge and hydrophobic surface has a stronger interaction force with the hydrophobic surface (i.e., TM-820 and SWC-5), and the succession detach in the force curve can be observed due to the polymer chains and bond rupture at the surface interface. This phenomenon is attributed to high heterogeneity of the membrane surface. On the other hand, the negatively charged CML particle is greatly affected by the membrane surface charge than the hydrophobicity, therefore the CML particle is favorable for adhering to the less negatively charged membrane surface. Fouling is contributed by two mechanisms (i.e., membrane-foulant and foulant–foulant interaction), and the only initial fouling step plays a significantly important role in the real RO plant. The initial fouling step can be compared with the interaction force since the initial fouling mechanism is able to be illustrated by the membrane-foulant interaction. The membrane which exposed the strongest interaction force with CML particle is less fouled in the flux test due to the electrical repulsion and vice versa. As a result, the proper membrane selection in the system according to the foulant is required for systematical management. A more detailed investigation should be carried out to obtain the database of the interaction force in terms of foulant versus membrane surface properties.

ACKNOWLEDGEMENT

The authors would like to thank the Ministry of Land, Transport, and Maritime Affairs (MLTM) for supporting this study through Seawater Engineering & Architecture of High Efficiency Reverse Osmosis (SEAHERO) program.

REFERENCES

1. Hong, S.; Elimelech, M. (1997) Chemical and physical aspects of natural organic matter (NOM) fouling of nanofiltration membranes. *Journal of Membrane Science*, 132: 159–181.
2. Brant, J.A.; Johnson, K.M.; Childress, A.E. (2006) Examining the electrochemical properties of a nanofiltration membrane with atomic force microscopy. *Journal of Membrane Science*, 276: 286–294.
3. Childress, A.E.; Deshmukh, S.S. (1998) Effect of humic substances and anionic surfactants on the surface charge and performance of reverse osmosis membranes. *Desalination*, 118: 167–174.

Downloaded At: 08:48 25 January 2011

4. Shim, Y.; Lee, H.J.; Lee, S.; Moon, S.H.; Cho, J. (2002) Effects of natural organic matter and ionic species on membrane surface charge. *Environmental Science & Technology*, 36: 3864–3871.
5. Lee, S.; Elimelech, M. (2006) Relating organic fouling of reverse osmosis membranes to intermolecular adhesion forces. *Environmental Science & Technology*, 40: 980–987.
6. Bowen, W.R.; Hial, N.; Lovitt, R.W.; Wright, C.J. (1998) A new technique for membrane characterization: Direct measurement of the force of adhesion of a single particle using an atomic force microscope. *Journal of Membrane Science*, 139: 269–274.
7. Yang, J.; Lee, S.; Lee, E.; Lee, J.; Hong, S. (2009) Effect of solution chemistry on the surface property of reverse osmosis membranes under seawater conditions. *Desalination*, 247: 148–161.
8. Marmur, A. (1996) Equilibrium contact angles: Theory and measurement. *Colloids and Surfaces A*, 116: 55–61.
9. Luxbacher, T. (2006) Electrokinetic characterization of flat sheet membranes by streaming current measurement. *Desalination*, 199: 376–377.
10. Mi, B.; Elimelech, M. (2008) Chemical and physical aspects of organic fouling of forward osmosis membranes. *Journal of Membrane Science*, 320: 292–302.
11. Portigliatti, M.; Koutsos, V.; Hervet, H.; Leger, L. (2000) Adhesion and deformation of a single latex particle. *Langmuir*, 16: 6374–6376.
12. Bowen, W.R.; Doneva, T.A.; Yin, H.B. (2002) Atomic force microscopy studies of membrane-solute interactions (fouling). *Desalination*, 146: 97–102.

Downloaded At: 08:48 25 January 2011